Performance Analysis of LDPC-Coded Diversity Combining on Rayleigh Fading Channels With Impulsive Noise

Zhen Mei, Martin Johnston, *Member, IEEE*, Stéphane Le Goff, and Li Chen, *Senior Member, IEEE*

***Abstract*— Spatial diversity is an effective method to mitigate the effects of fading, and when used in conjunction with low-density parity-check (LDPC) codes, it can achieve excellent error-correcting performance. Noise added at each branch of the diversity combiner is generally assumed to be additive white Gaussian noise, but there are many applications where the received signal is impaired by noise with a non-Gaussian distribution. In this paper, we derive the exact bit-error probability of different linear combining techniques on Rayleigh fading channels with impulsive noise, which is modeled using symmetric alpha-stable distributions. The relationship for the signal-to-noise ratios of these linear combiners is derived and then different non-linear detectors are presented. A detector based on the bi-parameter Cauchy–Gaussian mixture model is used and shows near-optimal performance with a significant reduction in complexity when compared with the optimal detector. Furthermore, the threshold signal-to-noise ratio of LDPC codes for different combining techniques on these channels is derived using density evolution and an estimation of the waterfall performance of LDPC codes is derived that reduces the gap between simulated and asymptotic performance.**

***Index Terms*— Impulsive noise, LDPC codes, diversity combining, finite length analysis.**

I. Introduction

DIVERSITY combining is an important technique that combats fading effects by exploiting spatial diversity. Traditional combining schemes such as maximal-ratio combining (MRC), equal-gain combining (EGC) and selection combining (SC) are chosen depending on the required trade-off between performance and complexity at the receiver. Conventionally, the noise added at each branch of the diversity combiner is assumed to be Gaussian. However, interference in wireless transceivers can exhibit an impulsive behavior [1], [2] and it is important to take this impulsive nature into account when analyzing spatial diversity. As an important class of heavy-tailed distributions, symmetric α-stable (SαS) distributions have successfully modeled multiple access interference in ad-hoc networks, near-field interference in wireless transceivers and underwater acoustic noise [3]–[5]. Nasri *et al* [6] have analyzed the asymptotic bit-error probability (BEP) of diversity combining schemes under general non-Gaussian noise with independent and identically distributed (i.i.d.) components, but this work cannot be applied to SαS distributions because they have an infinite variance. In [7]–[9], the statistics of interference from a field of Poisson distributed interferers modeled by SαS distribution was studied. The outage probability of diversity combining schemes for these applications was also derived [10]. For wireless channels with general SαS noise, Rajan and Tepedelenlioğlu [11] performed a diversity combining analysis for Rayleigh fading channels and complex isotropic SαS noise with dependent components, where diversity gain and asymptotic BEP were derived.

On the other hand, SαS noises with i.i.d. components have also been shown to be valid in some scenarios [5], [12], [13] and this type of channels is called the additive white SαS noise (AWSαSN) channel [14]. Optimal and sub-optimal detectors of AWSαSN channels were also widely investigated in the literature [15], [16]. Moreover, recently it was shown that if the passband sampling frequency f_s is four times the carrier frequency f_c, the components of the resulting SαS noise become independent and the system can be exploited to achieve the best error performance under maximum-likelihood (ML) detection [14]. Inspired by this, the detection of single-carrier and orthogonal frequency-division multiplexing (OFDM) systems was then presented [17], [18]. Moreover, this feature provides an elegant way to analyze the uncoded BEP over complex baseband SαS noise with i.i.d. real and imaginary components [19]. For fading channels with AWSαSN, linear combiners were compared in [20] and [21]. However, the analytic BEP has not been derived for different combiners on Rayleigh fading channels with AWSαSN, which will be addressed in this paper.

The performance of low-density parity-check (LDPC) codes with spatial diversity for additive white Gaussian noise (AWGN) channels has also been investigated in the literature [22], [23]. However, after a comprehensive survey of the literature, there appears to be no publications that have investigated the LDPC-coded performance of diversity combining on non-Gaussian channels. In this paper, we derive the asymptotic performance of LDPC codes with linear diversity combining

Manuscript received August 2, 2016; revised January 6, 2017; accepted March 10, 2017. Date of publication March 16, 2017; date of current version June 14, 2017. The associate editor coordinating the review of this paper and approving it for publication was G. Durisi. *(Corresponding author: Zhen Mei.)*

Z. Mei, M. Johnston, and S. Le Goff are with the School of Electrical and Electronic Engineering, Newcastle University, Newcastle upon Tyne NE1 7RU, U.K. (e-mail: z.mei@ncl.ac.uk; martin.johnston@ncl.ac.uk; stephane.le-goff@ncl.ac.uk).

L. Chen is with the School of Electronics and Information Technology, Guangdong Key Laboratory of Information Security, Sun Yat-sen University, Guangzhou 510006, China (e-mail: chenli55@mail.sysu.edu.cn).

Color versions of one or more of the figures in this paper are available online at http://ieeexplore.ieee.org.

Digital Object Identifier 10.1109/TCOMM.2017.2683485

schemes including SC, EGC and MRC on fading channels with non-Gaussian impulsive noise. Furthermore, to reduce the gap between the asymptotic and simulated performance of LDPC codes, we propose a waterfall performance analysis for LDPC codes on these channels. Of course, the asymptotic performance assumes infinite length LDPC codes so it is more useful if the performance of finite length LDPC codes can be estimated. In the literature, the finite length performance has only been investigated on binary symmetric channel (BSC), binary erasure channel (BEC) and AWGN channels [24]–[27], but in our paper, we extend the finite length performance analysis of AWGN channels in [26] to more general fading channels with impulsive noise.

The contributions of this paper are as follows: First, the analytic or semi-analytic BEPs of SC, EGC and MRC on Rayleigh fading channels with AWSαSN are derived. Moreover, the relationship for the performance of these combiners is derived, regardless of fading types. Second, the asymptotic and finite length performance of LDPC codes with different linear combiners on these channels is investigated for the first time in this paper. Finally, we compare different non-linear detectors and propose to use a detector based on the bi-parameter Cauchy-Gaussian mixture (BCGM) model [28] that achieves near-optimal performance at a much reduced complexity than the optimal detector on these channels.

This paper is organized as follows: Section II introduces SαS noise model and some important properties of SαS process. Section III derives the analytic and semi-analytic BEP for linear diversity combining schemes. Then the relationship for the dispersion of these combiners is derived. Moreover, optimal and sub-optimal non-linear detectors are presented and a near-optimal detector is proposed. Section IV derives the coded BEP, which consists of the asymptotic performance of LDPC codes with linear combiners and an estimation of the waterfall performance for finite length LDPC codes. In Section V, the decoding thresholds as well as numerical and simulation results are given. Finally, we conclude the paper in Section VI.

II. System and Channel Models

A. Channel Model and SαS Distributions

Consider a channel comprising multiple branches where the transmitted signal is received over L_r independent slowly-varying flat fading channels. Assuming perfect phase and timing synchronization, the received signal of the l-th branch can be modeled as

$$r_l = h_l x + n_l, \quad 1 \le l \le L_r, \tag{1}$$

where x is the modulated signal with binary phase-shift keying (BPSK) modulation. $h_l = a_l e^{j\phi_l}$ is the complex Gaussian channel gain, where a_l is the fading amplitude of the l-th branch with a Rayleigh probability density function (pdf) and ϕ_l is the phase of the h_l. We assume that $\{a_l\}_{l=1}^{L}$ are independent random variables with $\mathbb{E}[a_l^2] = 1$.

n_l is the complex noise where the real and imaginary components are i.i.d. and follow the univariate SαS distribution. The characteristic function of α-stable distributions is

$$\varphi(t) = \exp\left\{ j\delta t - |\gamma t|^{\alpha} (1 - j\beta \mathrm{sign}(t)\omega(t,\alpha)) \right\}. \tag{2}$$

where

$$\omega(t,\alpha) = \begin{cases} \tan(\pi\alpha/2), & \alpha \neq 1 \\ -2/\pi \log|t|. & \alpha = 1 \end{cases}$$

The α-stable distribution $S(\alpha, \beta, \gamma, \delta)$ in (2) has four parameters, α, β, γ and δ. 1) The characteristic exponent α, has a range $(0, 2]$ and controls the heaviness of the tail; 2) the skewness is denoted by β; 3) γ^{α} is known as the dispersion, which measures the spread of the pdf and is similar to the variance of a Gaussian distribution; 4) the location parameter is denoted as δ [29]. The α-stable distribution is called symmetric if β and δ are 0. Hence the pdf of a SαS distribution is defined as

$$f_{\alpha}(v;\gamma) = \frac{1}{2\pi} \int_{-\infty}^{\infty} e^{-|\gamma t|^{\alpha}} e^{-jtv} dt. \tag{3}$$

There are two special cases where the pdf of SαS distributions have closed-form expressions. When $\alpha = 2$, it follows a Gaussian distribution and the variance is related to the dispersion by $\sigma^2 = 2\gamma^2$. When $\alpha = 1$, the noise is Cauchy distributed. SαS distributed random variables have several useful properties, which are explained in [29] and [30]. Here we introduce three important properties that will be used in this paper:

Property 1: If $v_i \sim S(\alpha, 0, \gamma_i, 0)$, $i = 1, 2, \cdots, N$, then $\sum_{i=1}^{N} v_i \sim S(\alpha, 0, \gamma, 0)$, where $\gamma = \left(\sum_{i=1}^{N} \gamma_i^{\alpha}\right)^{\frac{1}{\alpha}}$.

Property 2: Let $v \sim S(\alpha, 0, \gamma, 0)$ and c is an arbitrary constant. Then $cv \sim S(\alpha, 0, |c|\gamma, 0)$.

Property 3: Any real SαS random variable $v \sim S(\alpha, 0, \gamma, 0)$ can be written as $v = \sqrt{B}G$, where B and G are independent, with $B \sim S(\alpha/2, 1, [\cos(\pi\alpha/4)]^{2/\alpha}, 0)$ and G is a Gaussian random variable with zero mean and variance σ^2.

According to Property 3, since components of n_l are mutually independent, the complex SαS noise can be described as

$$n_l = \sqrt{B_1} G_1 + j\sqrt{B_2} G_2, \tag{4}$$

where B_1 and B_2 are i.i.d. and are distributed like B. Similarly, G_1 and G_2 are i.i.d. Gaussian random variables which follow $\mathcal{N}(0, \sigma^2)$. The SαS noise is independent from channel to channel and independent of $\{h_l\}_{l=1}^{L}$. Hence, the instantaneous SNR of the l-th channel is given as $\eta_l = (a_l^2 E_s)/N_l$, where E_s is the symbol energy and N_l in the noise power in the l-th channel.

In practice, the noise parameters α and γ are not known. However, in the detection of SαS noise, the knowledge of parameters is very important since most detectors and decoders require this to achieve a good performance. Hence, the parameter estimation methods are needed. In the literature, algorithms based on sample fractiles [31], the extreme value theory [32] and empirical characteristic functions (ECFs) [33], have been proposed. In this paper, a fast estimation method proposed in [32] is used and the LDPC-coded performance with estimated parameters will be shown in Section V.

B. Geometric Signal-to-Noise Ratio

The conventional signal-to-noise ratio (SNR) is not defined for SαS noise since the second order moment of an SαS process does not exist. Hence we use the geometric SNR ($\mathrm{SNR_G}$) which is based on zero-order statistics [34]. $\mathrm{SNR_G}$ is defined as

$$\mathrm{SNR_G} = \frac{1}{2C_g}\left(\frac{A}{N_0}\right)^2, \tag{5}$$

where A is the amplitude of the modulated signal and $C_g \approx 1.78$ is the exponential of the Euler constant. The geometric power N_0 of the noise can be expressed as

$$N_0 = \frac{(C_g)^{1/\alpha}\gamma}{C_g}. \tag{6}$$

Hence the $\frac{E_b}{N_0}$ for a coded system with BPSK modulation is

$$\frac{E_b}{N_0} = \frac{1}{4R_c C_g^{(\frac{2}{\alpha}-1)}\gamma^2}, \tag{7}$$

where R_c is the code rate.

III. Uncoded BEP Analysis of Diversity Combining on Rayleigh Fading Channels With AWSαSN

In this section, the uncoded BEP of several linear diversity combining methods (SC, EGC and MRC) on Rayleigh fading channels with i.i.d. SαS noise will be derived analytically and semi-analytically.

First, we derive the uncoded BEP of a point-to-point system without fading. Similar to the Q-function, a right tail probability $Q_\alpha(x)$ is defined for SαS distributions as

$$Q_\alpha(x) = \int_x^\infty f_\alpha(t;1)dt, \tag{8}$$

where $f_\alpha(t;1)$ is the standard SαS distribution with $\gamma = 1$. In [19], the uncoded BEP was derived by only considering the Cauchy noise which is a special case. In this paper, we give a full derivation of BEP over general SαS noise as

$$\begin{aligned} P_{b,\alpha} &= P(x=+1)P(e|x=+1) + P(x=-1)P(e|x=-1) \\ &= \frac{1}{2}\int_{-\infty}^{0} f_\alpha(t-1;\gamma)dt + \frac{1}{2}\int_0^\infty f_\alpha(t+1;\gamma)dt \\ &= \int_1^\infty f_\alpha(u;\gamma)du, \end{aligned} \tag{9}$$

where e is a symbol error and $P(x=+1) = P(x=-1) = \frac{1}{2}$. According to the standardization of SαS random variables, if $x \sim S(\alpha,0,\gamma,0)$, then $x/\gamma \sim S(\alpha,0,1,0)$ and the pdf should be scaled by $1/\gamma$ [35]. Hence, (9) can be rewritten as

$$\begin{aligned} P_{b,\alpha} &= \int_1^\infty \frac{1}{\gamma} f_\alpha(\frac{u}{\gamma};1)du \\ &= \int_{\frac{1}{\gamma}}^\infty f_\alpha(v;1)dv \\ &= Q_\alpha\left(\frac{1}{\gamma}\right). \end{aligned} \tag{10}$$

Since geometric SNR is defined for the whole range of α, (10) is a general expression for all SαS channels. From (7) and (10), we can obtain $P_{b,\alpha}$ in terms of E_b/N_0 as

$$P_{b,\alpha} = Q_\alpha\left(\frac{1}{\gamma}\right) = Q_\alpha\left(\sqrt{4R_c C_g^{(\frac{2}{\alpha}-1)}\frac{E_b}{N_0}}\right). \tag{11}$$

When $R_c = 1$, (11) represents the BEP of an uncoded BPSK system on SαS channels.

From (8), a double integral must be evaluated to calculate $Q_\alpha(x)$, but there is an alternative representation of the cumulative distribution function (cdf) of SαS distributions given in [35] to reduce the complexity of calculating $Q_\alpha(x)$. Hence for SαS distributions with $x > 0$:

(a) When $\alpha \neq 1$,

$$Q_\alpha(x) = c_1 + \frac{\mathrm{sign}(\alpha-1)}{\pi}\int_0^{\frac{\pi}{2}} \exp\left(-x^{\frac{\alpha}{\alpha-1}}V(\theta;\alpha)\right)d\theta, \tag{12}$$

where

$$c_1 = \begin{cases} \frac{1}{2} & \alpha < 1 \\ 0 & \alpha > 1 \end{cases}$$

and

$$V(\theta;\alpha) = \left(\frac{\cos\theta}{\sin\alpha\theta}\right)^{\frac{\alpha}{\alpha-1}}\frac{\cos(\alpha-1)\theta}{\cos\theta}.$$

(b) When $\alpha = 1$,

$$Q_\alpha(x) = -\frac{1}{2} - \frac{1}{\pi}\arctan(x). \tag{13}$$

This new general expression of Q_α-function reduces the complexity of calculating $Q_\alpha(x)$ by replacing the double integral with a single integral.

A. Uncoded BEP of Selection Combining

For SC, the branch with the maximum SNR is chosen and the combined signal y is given as

$$y = \sum_{l=1}^{L_r} w_l r_l = w_k r_k, \tag{14}$$

where

$$w_k = \begin{cases} 1, & \text{if } \eta_k = \max\limits_l\{\eta_l\} \\ 0, & \text{otherwise} \end{cases},$$

and $\eta_l = a_l^2\frac{E_b}{N_0}$ is the output SNR of the l-th branch. Therefore, the combined signal can be rewritten as

$$y = h_{\mathrm{sc}}x + n_{\mathrm{sc}}, \tag{15}$$

where $h_{\mathrm{sc}} = a_{\mathrm{sc}}e^{j\phi_{\mathrm{sc}}}$ and n_{sc} are the channel gain and the noise of the branch with the largest output SNR, respectively. When fading effects are considered, (11) can be seen as a conditional BEP. For SC,

$$P_{b|a_{\mathrm{sc}},\alpha}(\eta) = Q_\alpha\left(\sqrt{4R_c C_g^{(\frac{2}{\alpha}-1)}\eta}\right), \tag{16}$$

where $\eta = a_{\text{sc}}^2 \frac{E_b}{N_0}$. Since h_{sc} is random, we need to average (16) over the pdf of η to obtain the unconditional BEP. Hence the analytic expression of the BEP for SC on Rayleigh fading channels with SαS noise is given as

$$P_{b,\alpha}^{\text{SC}} = \int_0^\infty P_{b|a_{\text{sc}},\alpha}(\eta)\, p(\eta;\overline{\eta}) d\eta = \int_0^\infty Q_\alpha\left(\sqrt{4R_c C_g^{(\frac{2}{\alpha}-1)}\eta}\right) p(\eta;\overline{\eta}) d\eta, \quad (17)$$

where $p(\eta;\overline{\eta})$ is the pdf of the output SNR η of SC and $\overline{\eta} = \frac{E_b}{N_0}$. For SC, the branch with the maximum SNR is chosen, hence the outage probability of SC with uncorrelated Rayleigh fading is given as

$$P_{\text{out}}(\eta_s) = P\left[\eta < \eta_s\right] = \prod_{l=1}^{L_r} P\left[\eta_l < \eta_s\right] = \left(1 - e^{-\eta_s/\overline{\eta}}\right)^{L_r}. \quad (18)$$

$P_{\text{out}}(\eta_s)$ represents the cdf of the output SNR as a function of the threshold η_s. Hence, the pdf of the output SNR of SC can be calculated by differentiating (18). The resulting pdf is given as

$$p(\eta;\overline{\eta}) = \frac{dP_{\text{out}}(\eta)}{d\eta} = \frac{L_r}{\overline{\eta}} e^{-\eta/\overline{\eta}} \left(1 - e^{-\eta/\overline{\eta}}\right)^{L_r - 1}. \quad (19)$$

By substituting (19) to (17), the analytic BEP for SC can be obtained.

B. Uncoded BEP of Equal-Gain Combining

For EGC, all channels have a unit gain and the combined signal y is obtained by dividing the received signal r_l by the phase of h_l:

$$y = \sum_{l=1}^{L_r} e^{-j\phi_l} r_l = x \sum_{l=1}^{L_r} a_l + \sum_{l=1}^{L_r} \tilde{n}_l, \quad (20)$$

where $\tilde{n}_l = n_l e^{-j\phi_l}$. Similar to SC, the combined signal y in (20) can be rewritten as

$$y = a_{\text{egc}} x + n_{\text{egc}}, \quad (21)$$

where $a_{\text{egc}} = \sum_{l=1}^{L_r} a_l$ and $n_{\text{egc}} = \sum_{l=1}^{L_r} \tilde{n}_l$. We note that $\tilde{n}_l = n_l e^{-j\phi_l}$ is still SαS distributed with the same α and γ as n_l. The proof is given in the Appendix A. Then according to Property 1, $n_{\text{egc}} \sim S(\alpha, 0, \gamma_{\text{egc}}, 0)$, where the dispersion of n_{egc} is calculated as

$$\gamma_{\text{egc}} = L_r^{1/\alpha} \gamma. \quad (22)$$

Since a_{egc} is random, the conditional BEP for EGC is given as

$$P_{b|a_{\text{egc}},\alpha} = Q_\alpha\left(L_r^{-\frac{1}{\alpha}} \sqrt{4R_c C_g^{(\frac{2}{\alpha}-1)} \frac{a_{\text{egc}}^2 E_b}{N_0}}\right) = Q_\alpha\left(a_{\text{egc}} L_r^{-\frac{1}{\alpha}} \sqrt{4R_c C_g^{(\frac{2}{\alpha}-1)} \frac{E_b}{N_0}}\right). \quad (23)$$

Hence the analytic BEP for EGC on Rayleigh fading channels with SαS noise is calculated as

$$P_{b,\alpha}^{\text{EGC}} = \int_0^\infty P_{b|a_{\text{egc}},\alpha}\, p(a_{\text{egc}}) da_{\text{egc}} = \int_0^\infty Q_\alpha\left(a_{\text{egc}} L_r^{-\frac{1}{\alpha}} \sqrt{4R_c C_g^{(\frac{2}{\alpha}-1)} \frac{E_b}{N_0}}\right) p(a_{\text{egc}}) da_{\text{egc}}, \quad (24)$$

where $p(a_{\text{egc}})$ is the pdf of the output channel gain a_{egc} of EGC. The exact pdf of a_{egc} cannot be given in closed-form, but accurate closed-form approximations of Rayleigh sum distributions were proposed in [36] and [37] and in this paper, we use these models to find $p(a_{\text{egc}})$. When $L_r = 2$, a small argument approximation (SAA) proposed in [36] is used and the pdf of a_{egc} is given as

$$p(a_{\text{egc}}) = \frac{a_{\text{egc}}^{(2L_r-1)} e^{-\frac{a_{\text{egc}}^2}{2b}}}{2^{L_r-1} b^{L_r} (L_r - 1)!}, \quad (25)$$

where

$$b = \frac{\sigma^2}{L_r} \left(\prod_{x=1}^{L_r} (2x-1)\right)^{1/L_r}.$$

When $L_r \geq 3$, an accurate closed-form approximation is given in (26), as shown at the bottom of this page. The values of a_0, a_1 and a_2 for different L_r can be found in [37]. We note that the standard deviation σ for Rayleigh distributions in the calculation of b should be normalized as $\sigma = \sqrt{\frac{L_r}{2}}$.

C. Uncoded BEP of Maximal-Ratio Combining

The maximal ratio combiner does not exist for SαS noise when $\alpha \neq 2$ since the second order moment of alpha-stable process is infinite [29]. Therefore, the MRC in this paper only refers to particular weights and the pdf of the output SNR cannot be obtained.

To find the BEP of MRC, a different approach must be applied. The combined signal is divided by $\sum_{l=1}^{L_r} w_l a_l$ and since the weights are chosen as $w_l = h_l^* = a_l e^{-j\phi_l}$ for MRC, it becomes

$$\hat{y} = x + \hat{n}, \quad (27)$$

$$p(a_{\text{egc}}) = \frac{a_{\text{egc}}^{(2L_r-1)} e^{-\frac{a_{\text{egc}}^2}{2b}}}{2^{L_r-1} b^{L_r} (L_r-1)!} - \frac{(a_{\text{egc}} - a_2)^{(2L_r-2)} e^{-\frac{a_1 (a_{\text{egc}} - a_2)^2}{2b}}}{2^{(L_r-1)} b \left(\frac{b}{a_1}\right)^{L_r} (L_r-1)!} \times a_0 \left[b(2L_r a_{\text{egc}} - a_2) - a_1 a_{\text{egc}} (a_{\text{egc}} - a_2)^2\right] \quad (26)$$

where

$$\hat{y} = \frac{y}{\sum_{l=1}^{L_r} a_l^2} \tag{28}$$

and

$$\hat{n} = \frac{\sum_{l=1}^{L_r} a_l e^{-j\phi_l} n_l}{\sum_{l=1}^{L_r} a_l^2}. \tag{29}$$

We note that the BEP will not change if we divide y by a positive constant and $\hat{n}$ is still an SαS random variable but with a different value of dispersion. According to Properties 1 and 2, the dispersion of $\hat{n}$ is given as

$$\gamma_{\text{mrc}} = \left(\sum_{l=1}^{L_r} \left| \frac{a_l e^{-j\phi_l}}{\sum_{l=1}^{L_r} a_l^2} \right|^{\alpha} \right)^{\frac{1}{\alpha}} \quad \gamma = \frac{\left(\sum_{l=1}^{L_r} a_l^{\alpha} \right)^{\frac{1}{\alpha}}}{\sum_{l=1}^{L_r} a_l^2} \gamma \tag{30}$$

The conditional BEP can be obtained by substituting (30) and (7) into (11). The result is expressed as

$$P_{b|a_{\text{mrc}},\alpha} = Q_{\alpha} \left(\omega \sqrt{4 R_c C_g^{(\frac{2}{\alpha}-1)} \frac{E_b}{N_0}} \right), \tag{31}$$

where

$$\omega = \frac{\sum_{l=1}^{L_r} a_l^2}{\left(\sum_{l=1}^{L_r} a_l^{\alpha} \right)^{\frac{1}{\alpha}}}. \tag{32}$$

The pdf of ω cannot be evaluated as an analytic expression, hence we adopt a Monte-Carlo simulation and histogram method to find $p(\omega)$. Finally, the semi-analytic BEP of MRC on Rayleigh fading channels with SαS noise is

$$P_{b,\alpha}^{\text{MRC}} = \int_0^{\infty} Q_{\alpha} \left(\omega \sqrt{4 R_c C_g^{(\frac{2}{\alpha}-1)} \frac{E_b}{N_0}} \right) p(\omega) d\omega. \tag{33}$$

D. Performance Comparison of Linear Combiners

The SNR advantage of optimal linear combiners over MRC and EGC was presented in [20] and [21]. In this subsection, the noise power of SC, EGC and MRC are compared to give an insight into the performance of different combiners. Similar to MRC, (15) and (21) can also be rewritten as $\hat{y} = x + \hat{n}$ with no change on the BEP. $\hat{n} = n_{\text{sc}}/h_{\text{sc}}$ for SC and $\hat{n} = n_{\text{egc}}/a_{\text{egc}}$ for EGC. In this case, the dispersions of the noise for SC and EGC are given as

$$\hat{\gamma}_{\text{sc}} = \frac{1}{a_m} \gamma \quad \text{and} \quad \hat{\gamma}_{\text{egc}} = \frac{L_r^{1/\alpha}}{\sum_{l=1}^{L_r} a_l} \gamma, \tag{34}$$

where $a_m = \max\{a_1, a_2, \cdots, a_{L_r}\}$. The relationship of the dispersion between these three combiners is given as

(a) When $0 < \alpha \leq 1$,

$$\hat{\gamma}_{\text{sc}} \leq \gamma_{\text{mrc}} \leq \hat{\gamma}_{\text{egc}} \leq L_r^{\frac{1}{\alpha}} \hat{\gamma}_{\text{sc}}, \tag{35}$$

(b) When $1 \leq \alpha < 2$,

$$L_r^{\frac{1}{\alpha}-1} \hat{\gamma}_{\text{sc}} \leq \gamma_{\text{mrc}} \leq \hat{\gamma}_{\text{egc}} \leq L_r^{\frac{1}{\alpha}} \hat{\gamma}_{\text{sc}}. \tag{36}$$

We note that the relationships in (35) and (36) are independent of fading types. The proof of (35) and (36) is given in the Appendix B. According to (6), the noise power is proportional to the dispersion of the noise. (35) and (36) imply that MRC always performs better than EGC regardless of the fading type. Particularly, SC shows the best performance when the channel is extremely impulsive ($\alpha < 1$). Moreover, according to (35) and (36), the upper bound and lower bound of the performance for MRC and EGC can be determined by SC. The SNR of these combiners can be easily compared and the numerical results will be given in Section V-A.

E. Optimal and Sub-Optimal Detectors

Although linear combiners are simple, they do not consider the degradation caused by impulsive interference. As shown in the literature, non-linear detectors can achieve better performance [15], [21] on impulsive noise channels. The decision metric of the optimal detector is given as

$$\lambda_{\text{op}} = \sum_{l=1}^{L_r} \ln \frac{P(x_l = +1 | r_l, a_l)}{P(x_l = -1 | r_l, a_l)} = \sum_{l=1}^{L_r} \ln \frac{f_{\alpha}(r_l - a_l; \gamma)}{f_{\alpha}(r_l + a_l; \gamma)}. \tag{37}$$

We note that (37) gives the initial log-likelihood ratios (LLRs) for soft-input-soft-output decoding.

The complexity in calculating (37) is very high since the pdf of SαS distributions is not given in closed-form, so sub-optimal detectors are required to reduce the complexity. In the literature, the Cauchy detector has been shown to achieve a good performance for a large range of α, especially when α approaches one [38]. The Cauchy detector can be expressed as

$$\lambda_{\text{Cauchy}} = \sum_{l=1}^{L_r} \ln \left(\frac{\gamma^2 + (y_l + a_l)^2}{\gamma^2 + (r_l - a_l)^2} \right). \tag{38}$$

However, the Cauchy detector leads to a significant degradation when the channel is only slightly impulsive (α is close to two), since Cauchy distribution is only a special case of SαS distributions at $\alpha = 1$. In order to better approximate SαS distributions, two classes of mixture models were proposed. One is Gaussian mixture model (GMM) which is the sum of a finite number of scaled Gaussian pdf. However, GMM cannot accurately capture the tail behavior of SαS distributions. The other is Cauchy-Gaussian mixture (CGM) model which utilizes the algebraic tail of Cauchy distribution. CGM model is a multiplicative mixture of a Cauchy pdf and a Gaussian pdf, but require three parameters: mixture ratio ϵ, the scale parameter γ and the variance σ^2 of the Gaussian distribution. The BCGM model is a new type of CGM models with only two parameters, a mixture ratio ϵ and γ, and it approximates SαS pdf well at $\alpha \in [1, 2]$ [28]. In this paper, we use this BCGM model to achieve near-optimal performance. The BCGM pdf is given as

$$f_{\text{CG}}(x; \gamma) = (1 - \epsilon) \frac{1}{2\sqrt{\pi}\gamma} \exp\left(-\frac{x^2}{4\gamma^2} \right) + \epsilon \frac{\gamma}{\pi(x^2 + \gamma^2)}. \tag{39}$$

A near-optimum value is achieved when

$$\varepsilon = \frac{2\Gamma(-\omega/\alpha) - \alpha\Gamma(-\omega/2)}{2\alpha\Gamma(-\omega) - \alpha\Gamma(-\omega/2)}, \tag{40}$$

where the gamma function is defined as $\Gamma(x) = \int_0^\infty e^{-t}t^{x-1}dt$ and $\omega < \alpha$. The BCGM detector can be obtained by replacing the SαS pdf in (37) by (39). We note that the BCGM is only valid when $\alpha \in [1, 2]$ and when $\alpha < 1$, the BCGM detector reduces to a Cauchy detector. The complexity of this new detector is much lower than the optimal detector since its pdf is given in closed-form. The uncoded and coded performance of optimal and sub-optimal detectors will be examined in Section V.

IV. Coded BEP Analysis for Linear Diversity Combining Techniques

A. Asymptotic Performance of LDPC Codes

The ensemble of LDPC codes can be represented by a bipartite graph comprising variable nodes and check nodes. A regular LDPC code ensemble can be defined by a degree pair (d_v, d_c), where d_v and d_c are the number of edges incident to each variable node and check node, respectively. An irregular LDPC code can be characterized by edge degree distributions $\lambda(x)$ and $\rho(x)$, which are defined as

$$\lambda(x) = \sum_{j\geq 2} \lambda_j x^{j-1}, \quad \rho(x) = \sum_{i\geq 2} \rho_i x^{i-1}. \tag{41}$$

λ_j and ρ_i are the fraction of edges that are connected to variable and check nodes with degree j and i, respectively.

Several methods such as density evolution (DE), Gaussian approximation (GA) and extrinsic information transfer (ExIT) charts have been proposed to find the asymptotic performance of LDPC codes [39]–[41]. However, only DE is valid for general binary memoryless symmetric channels (BMSC) and it is employed in this paper to calculate the threshold of a specific ensemble of LDPC codes. In this section, we will show how to apply DE to diversity combining techniques on i.i.d. Rayleigh fading channels with additive SαS noise.

1) Initial PDF of Log-Likelihood Ratio (LLR): DE tracks the pdf of LLRs during the iterative decoding process. To start the process of DE, the initial pdf of the LLRs must be calculated. Assuming we have perfect side information, the initial LLR of the decoder for SC or EGC is calculated as

$$v^{(0)} = \ln \frac{P(x=+1|y,a)}{P(x=-1|y,a)} = \ln \frac{f_\alpha(y-a;\gamma)}{f_\alpha(y+a;\gamma)}, \tag{42}$$

where a is the combining channel gain over i.i.d. Rayleigh fading channels, which is denoted as a_{sc} or a_{egc} for SC or EGC, respectively. Similarly, γ becomes γ_{egc} for EGC. The pdf of (42) has no analytic expression with the exception of $\alpha = 2$ and Monte-Carlo simulations with a histogram method are used to obtain the conditional pdf of $v^{(0)}$ as $p(v^{(0)}|a)$. To obtain the unconditional density function of $v^{(0)}$, we need to average $p(v^{(0)}|a)$ over the pdf of a as

$$p_v^{(0)} = \int_0^\infty p(v^{(0)}|a)p(a)da, \tag{43}$$

where $p(a)$ is the pdf of the combining channel gain a.

To derive the pdf of a_{sc} for SC, we change the variable of (19), a_{sc}, using the relationship $p(\eta)d\eta = p(a_{\text{sc}})da_{\text{sc}}$ and $a_{\text{sc}}^2 = \eta/\overline{\eta}$. Hence, the pdf of a is expressed as

$$p(a_{\text{sc}}) = 2a_{\text{sc}}L_r e^{-a_{\text{sc}}^2}\left(1-e^{-a_{\text{sc}}^2}\right)^{L_r-1}. \tag{44}$$

For EGC, the closed-form approximated pdf of a_{egc} has been given in (26). Alternatively, a simulation-based approach can be used to find the pdf of a_{egc} using a histogram method.

For MRC, a different approach is used to find the pdf of the initial LLR. According to (27) and (30), the initial LLR can be written as

$$v^{(0)} = \ln \frac{f_\alpha(\hat{y}-1;\gamma_{\text{mrc}})}{f_\alpha(\hat{y}+1;\gamma_{\text{mrc}})}. \tag{45}$$

The relationship between γ_{mrc} and γ has been derived in (30), $\gamma_{\text{mrc}} = \xi\gamma$, where ξ is a random variable and is expressed as

$$\xi = \frac{\left(\sum_{l=1}^{L_r} a_l^\alpha\right)^{\frac{1}{\alpha}}}{\sum_{l=1}^{L_r} a_l^2}. \tag{46}$$

Hence the unconditional pdf of $v^{(0)}$ is obtained as

$$p_v^{(0)} = \int_0^\infty p(v^{(0)}|\xi)p(\xi)d\xi, \tag{47}$$

where $p(\xi)$ is the pdf of ξ, which cannot be given in a closed-form. Similarly, a simulation-based approach is used to find $p(\xi)$.

2) Density Evolution Analysis: After initialization, DE of the sum-product algorithm (SPA) is a two-stage iterative process which consists of DE for the check node update and variable node update. With the initial LLR pdf $p_v^{(0)}$ obtained, the DE of the check node update is given as

$$p_u^{(l)} = \Lambda^{-1}\left(\sum_{i\geq 2}\rho_i\left(\Lambda\left[p_v^{(l-1)}\right]\right)^{\otimes(i-1)}\right), \tag{48}$$

where $\otimes$ represents the convolution operation, $p_u^{(l)}$ is the pdf of each check node output and $p_v^{(l)}$ is the pdf of each variable node output at the l-th iteration. Λ and Λ^{-1} are the changes in density due to $g(\cdot)$ and $g^{-1}(\cdot)$ respectively, where

$$g(z) = \left(\text{sign}(z), \ln\coth|z/2|\right). \tag{49}$$

The DE of the variable node update is expressed as

$$p_v^{(l)} = p_v^{(0)} \otimes \sum_{j\geq 2}\lambda_i\left(p_u^{(l)}\right)^{\otimes(j-1)}. \tag{50}$$

The summations in the variable node update become convolutions in (50). We assume that the all-zero codeword ($x = +1$) is transmitted, hence the fraction of incorrect messages for the l-th iteration can be denoted as

$$P_e^{(l)} = \int_{-\infty}^0 p_v^{(l)}(x)dx. \tag{51}$$

For a given noise parameter γ, this two-stage iterative algorithm is performed until the error probability either converges to zero or stops at a certain value. The threshold γ^* of a specific ensemble of LDPC codes is the supremum of all γ such that $P_e^{(l)}$ converges to zero as the number of iterations tends to infinity:

$$\gamma^* = \sup\left\{\gamma : \lim_{l\to\infty}\int_{-\infty}^0 p_v^{(l)}(x)dx = 0\right\}. \tag{52}$$

The threshold γ^* indicates where the waterfall region begins which allows us to estimate the performance of LDPC codes. However, since DE assumes the code length is infinite and cycle-free, there is still a gap between the threshold and actual performance of LDPC codes.

B. Waterfall Performance Estimation of LDPC Codes

In the asymptotic analysis of LDPC codes, the channel quality of transmitting each codeword is fixed since it assumes the codeword has an infinite length. However, for finite-length LDPC codes, the channel variation for each codeword should be considered. In this subsection, we extend the analysis in [26] to more general non-Gaussian channels by using DE rather than GA. An accurate estimation of block and bit-error probability of finite length LDPC codes on Rayleigh fading channels with SαS is given by observing the real-time channel quality.

First, we define $P_{b,\alpha}^{\text{obs}}$ as the observed bit-error rate (BER) of any received codeword of length N, which is a random variable. Then the number of errors $NP_{b,\alpha}^{\text{obs}}$ in a codeword follow a binomial distribution $B(N, P_{b,\alpha})$ [26]. $P_{b,\alpha}^{c}$ is the probability of a bit error and is denoted as either $P_{b,\alpha}^{\text{SC}}$, $P_{b,\alpha}^{\text{EGC}}$ or $P_{b,\alpha}^{\text{MRC}}$, depending on the type of combiner. When N is large, the pmf of $NP_{b,\alpha}^{\text{obs}}$ can be approximated by a normal distribution $\mathcal{N}(NP_{b,\alpha}^{c}, NP_{b,\alpha}^{c}(1-P_{b,\alpha}^{c}))$. Hence, the pdf of $P_{b,\alpha}^{\text{obs}}$ is given by $\mathcal{N}(P_{b,\alpha}^{c}, P_{b,\alpha}^{c}(1-P_{b,\alpha}^{c})/N)$. Then the block-error probability of LDPC codes with ensemble (λ, ρ) is calculated as

$$P_{\text{B}}^{\alpha}(N,\lambda,\rho) = \int_{P_{\text{th}}}^{1} f_{P_{b,\alpha}^{\text{obs}}}(N,x)dx = Q\left(\frac{P_{\text{th}} - \mu_{P_{b,\alpha}^{\text{obs}}}}{\sigma_{P_{b,\alpha}^{\text{obs}}}}\right), \tag{53}$$

where $\mu_{P_{b,\alpha}^{\text{obs}}} = P_{b,\alpha}^{c}$ and $\sigma_{P_{b,\alpha}^{\text{obs}}} = P_{b,\alpha}^{c}(1-P_{b,\alpha}^{c})/N$. P_{th} is the corresponding BEP of the threshold SNR $\left(\frac{E_b}{N_0}\right)_{\text{th}}$ and the block-error probability is $P_{b,\alpha}^{\text{obs}} > P_{\text{th}}$.

The threshold SNR $\left(\frac{E_b}{N_0}\right)_{\text{th}}$ can be calculated from γ^* which has been obtained in the previous section. Hence for SC, EGC and MRC, P_{th} can be found by substituting $\left(\frac{E_b}{N_0}\right)_{\text{th}}$ into (17), (24) and (33), respectively.

The coded BEP $P_{\text{b}}^{\alpha}(N,\lambda,\rho)$ can be derived from $P_{\text{B}}^{\alpha}(N,\lambda,\rho)$. According to DE, we observe that the decoder has a probability $P_e^{(l_{\max})}$ of failing, where $l_{\max}$ is the maximum number of iterations when DE is performed. This probability does not change significantly when the channel is slightly worse than the threshold. Each codeword has a probability $P_{\text{B}}^{\alpha}(N,\lambda,\rho)$ of being in error, hence the estimated coded BEP is given as

$$P_{\text{b}}^{\alpha}(N,\lambda,\rho) = P_e^{(l_{\max})} P_{\text{B}}^{\alpha}(N,\lambda,\rho). \tag{54}$$

V. Results and Discussion

A. SNR Comparison

To verify our SNR analysis of SC, EGC and MRC in Section III-D, the SNR gain of SC over EGC and MRC is presented in Fig. 1. We note that the SNR gain over EGC and MRC is given as $20\log_{10}(\hat{\gamma}_{\text{egc}}/\hat{\gamma}_{\text{sc}})$ and $20\log_{10}(\gamma_{\text{mrc}}/\hat{\gamma}_{\text{sc}})$, respectively. It is shown that MRC always performs better than EGC, which agrees with (35) and (36). Moreover, we observe that SC has the best performance for small values of α. However, it degrades as α increases and starts to have no gain over MRC and EGC from $\alpha = 1.3$ and $\alpha = 1.55$, respectively. We note that the SNR comparison of different combiners give a good insight into their performance. In the following subsections, observations from Fig. 1 will be verified by results of uncoded and coded BEP performance.

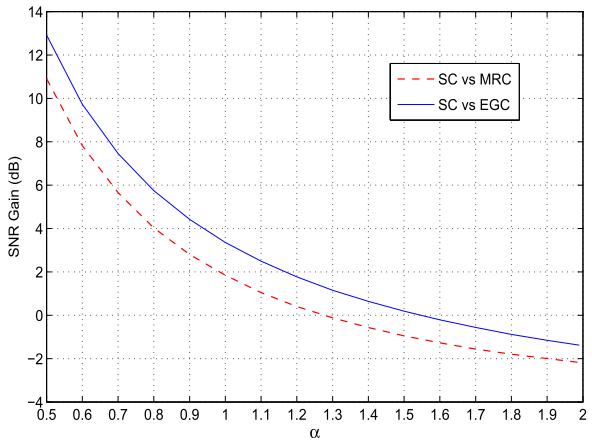

Fig. 1. SNR gain of SC over EGC and MRC with different α for $L_r = 3$.

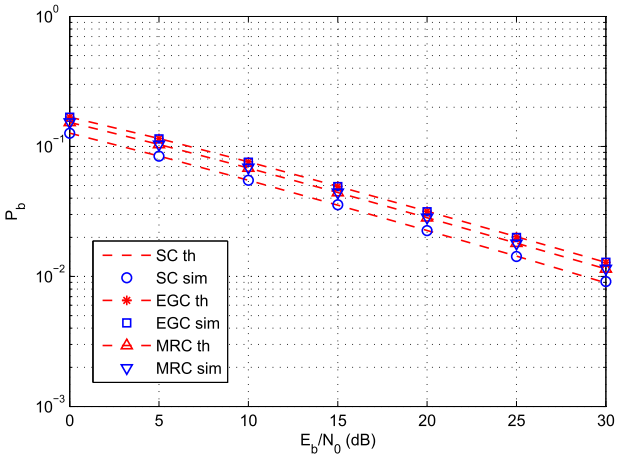

Fig. 2. Uncoded BEP of SC, EGC and MRC with $L_r = 2$ on Rayleigh fading channels with SαS noise at $\alpha = 0.8$.

B. Uncoded BEP

In this subsection, both the analytic and simulated performance of different combining methods with different levels of impulsiveness are investigated. In addition to this, the performance of optimal and sub-optimal detectors are presented. As shown in Fig. 2 - 4, the analytic BEP matches well with simulated BER for SC, EGC and MRC with different α ($\alpha = 0.8, 1.4, 1.9$) and different number of branches ($L_r = 2, 3, 4$).

As seen in Fig. 2, when compared with the other two linear diversity combining techniques, SC achieves the best

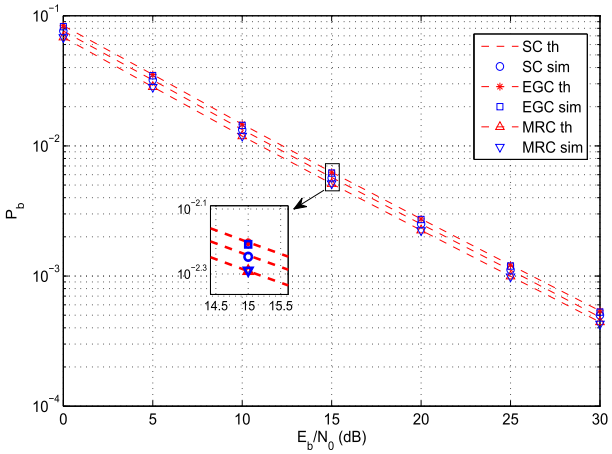

Fig. 3. Uncoded BEP of SC, EGC and MRC with $L_r = 3$ on Rayleigh fading channels with SαS noise at $\alpha = 1.4$.

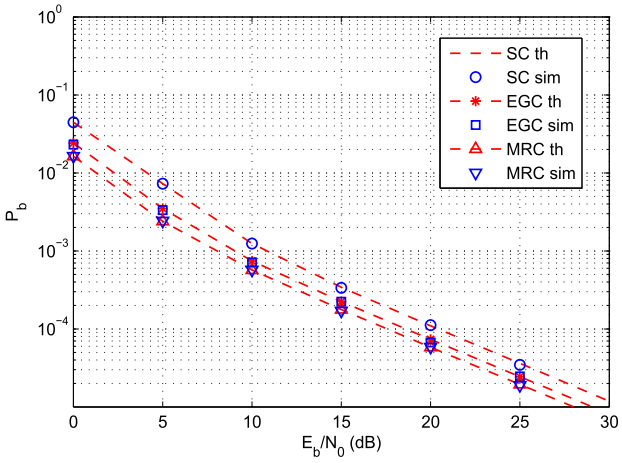

Fig. 4. Uncoded BEP of SC, EGC and MRC with $L_r = 4$ on Rayleigh fading channels with SαS noise at $\alpha = 1.9$.

performance at small values of α ($\alpha = 0.6$) and this result agrees with the observations in [21]. At the same SNR, the relationship of the BEP for SC, EGC and MRC is $P_{b,\alpha}^{\mathrm{SC}} < P_{b,\alpha}^{\mathrm{MRC}} < P_{b,\alpha}^{\mathrm{EGC}}$. As the channel becomes less impulsive ($\alpha = 1.4$), the performance of SC degrades when compared with EGC and MRC and we have $P_{b,\alpha}^{\mathrm{MRC}} < P_{b,\alpha}^{\mathrm{SC}} < P_{b,\alpha}^{\mathrm{EGC}}$, which verifies our observation in Fig. 1 that SC starts to perform worse than MRC and EGC at $\alpha = 1.3$ and $\alpha = 1.55$ since $1.3 < 1.4 < 1.55$. When $\alpha = 1.9$, SC shows the worst performance among the three linear diversity combining techniques and $P_{b,\alpha}^{\mathrm{MRC}} < P_{b,\alpha}^{\mathrm{EGC}} < P_{b,\alpha}^{\mathrm{SC}}$. We observe that SC can achieve superior performance when the effect of impulses is strong and the performance degrades as α increases. Although MRC only uses a particular set of weights, when compared with SC and EGC it can still achieve a good performance especially when α is close to two. We note that the BEP we obtained in Fig. 2 - 4 shows good agreement with our numerical results for the SNR comparison in Fig. 1.

The performance of optimal, Cauchy and BCGM detectors are presented in Fig. 5. When the channel is extremely impulsive, the BCGM detector reduces to the Cauchy detector

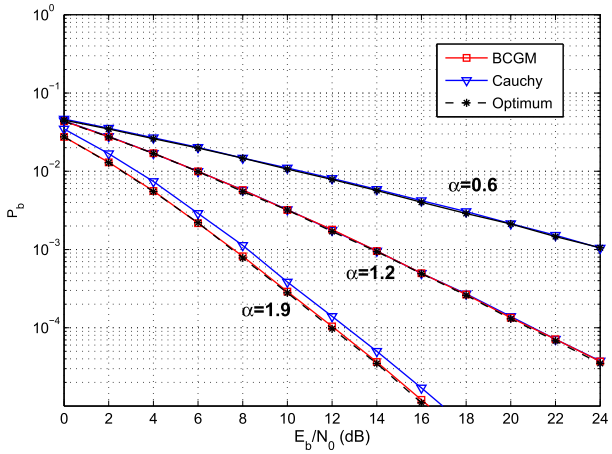

Fig. 5. Performance of different detectors with $L_r = 3$ on Rayleigh fading channels with SαS noise at $\alpha = 1.9$ and $\alpha = 1.2$.

TABLE I

THE THRESHOLD SNRS IN DB OF REGULAR LDPC CODES WITH SC, EGC AND MRC FOR RAYLEIGH FADING CHANNELS WITH SαS NOISE

	$L_r = 2$			$L_r = 4$		
	SC	EGC	MRC	SC	EGC	MRC
$\alpha = 1.8$	0.91	0.52	-0.18	-1.02	-2.31	-3.43
$\alpha = 1.4$	1.90	2.44	1.53	-0.19	0.37	-0.98
$\alpha = 1$	3.02	5.32	4.10	0.92	4.93	3.16
$\alpha = 0.6$	4.32	10.55	9.15	2.17	14.31	12.10

and it is shown that the Cauchy detector achieves near-optimal performance at $\alpha = 0.6$. When α approaches one ($\alpha = 1.2$), both Cauchy and BCGM detectors achieve near-optimal performance. However, when the channel is only slightly impulsive, the gap between the optimal detector and Cauchy detector becomes larger. When $\alpha = 1.9$ and $L_r = 3$, the optimum detector shows a gain of about 0.8 dB when compared with the Cauchy detector. In contrast, our proposed BCGM detector shows almost optimal performance in all situations.

C. Coded BEP

In this subsection, the asymptotic and finite length performance of regular and irregular LDPC codes are evaluated with both numerical and simulation results. The rate 1/2 regular (3,6) LDPC codes and the irregular LDPC codes with degree distribution of $\lambda(x) = 0.4x^2 + 0.4x^5 + 0.2x^8$, $\rho(x) = x^8$ are used. The block lengths considered are $N = 1000, 4000, 20000$ bits. For short or moderate length LDPC codes ($N \leq 4000$), the progressive edge-growth (PEG) algorithm is used to maximize the local girth [42]. For long LDPC codes ($N = 20000$), random construction is employed since the complexity of PEG is very high.

Table I shows the threshold SNRs of $(3, 6)$ regular LDPC codes with SC, EGC and MRC for spatial diversity systems. The relationship of asymptotic performance of LDPC codes we obtained for these combiners show good agreement with the uncoded performance we analyzed for different linear

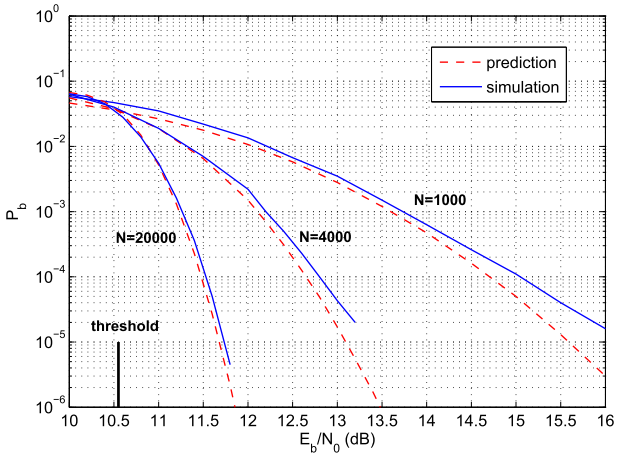

Fig. 6. Performance of regular $(3, 6)$ LDPC codes with EGC for $N = 1000, 4000, 20000$ at $L_r = 2$ on Rayleigh fading channels with SαS noise at $\alpha = 0.6$.

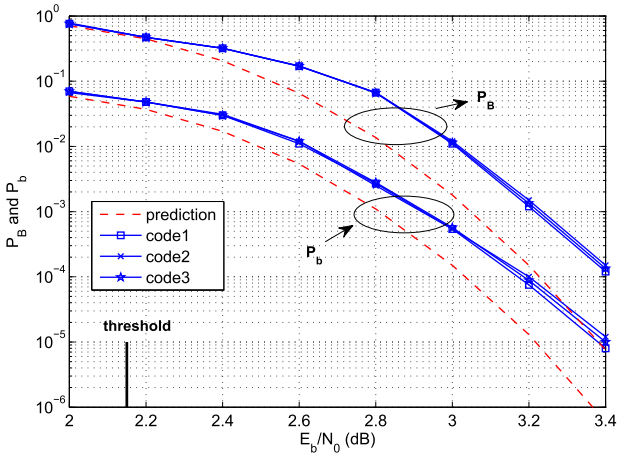

Fig. 7. Performance of irregular LDPC codes with SC at $L_r = 2$ and $N = 4000$ on Rayleigh fading channels with SαS noise at $\alpha = 1.5$.

combiners. As shown in Table I, SC shows the best performance for very impulsive noise channels ($\alpha = 0.6$ and $\alpha = 1$) for $L_r = 2$ and $L_r = 4$. When the channel is moderately impulsive ($\alpha = 1.4$), MRC starts to outperform SC and as the channel becomes less impulsive, the gap between MRC and SC becomes larger. For example, the threshold SNR of MRC is 1.53 dB at $\alpha = 1.4$ and $L_r = 2$, which is 0.37 dB smaller than SC. When $\alpha = 1.8$, the difference increases to 1.09 dB. EGC only shows a good performance for slightly impulsive channels ($\alpha = 1.8$).

Moreover, an interesting observation is that more branches do not always give better performance when impulses are present. As illustrated in Table I, as α decreases, $L_r = 4$ achieves a smaller gain than $L_r = 2$ for EGC and MRC, respectively. When $\alpha = 0.6$, the thresholds of EGC and MRC for $L_r = 4$ are even larger than for $L_r = 2$. This implies that very severe impulses will lead to a larger degradation with EGC and MRC when there are more branches, which means that the received signals from other branches become a source of interference.

In addition to the results of the asymptotic analysis given in Table I, the waterfall performance estimation and simulation results for both regular and irregular LDPC codes are presented in Figs. 6 - 9. As shown in Fig. 6, our estimated results match the simulation results closely with EGC at $\alpha = 0.6$ which is extremely impulsive. We observe a reduction in the gap between the estimated and simulation results as the block length N increases. The estimated performance inaccuracy decreases from 0.3 dB to 0.15 dB as N increases from 1000 to 4000. When $N = 20000$, the analytic and simulated performance are almost identical. We note that even for very long LDPC codes ($N = 20000$), the gap between the threshold SNR and simulation results is about 2.3 dB which is much larger than our estimated results.

Fig. 7 presents the simulated block and bit error rates of irregular LDPC codes with $N = 4000$, when the channel is moderately impulsive. Here, three different LDPC codes are constructed from the same degree distribution and their performance is evaluated to show the generalization of our

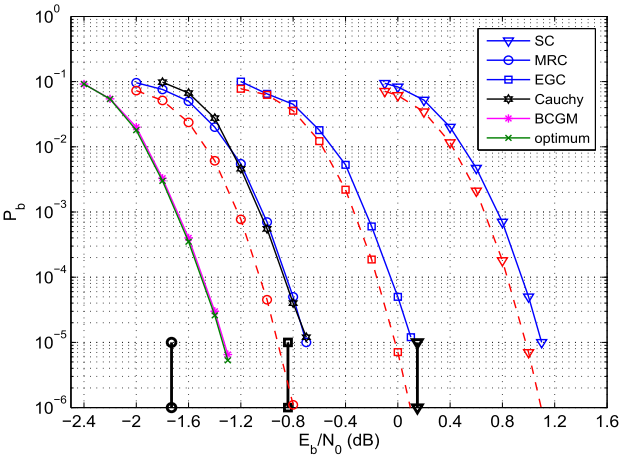

Fig. 8. Performance of irregular LDPC codes with different combiners at $L_r = 3$ and $N = 4000$ on Rayleigh fading channels with SαS noise at $\alpha = 1.8$.

method. The performance is accurately estimated by our analytic P_B and P_b in (53) and (54) with a 0.2 dB difference at the error rate of 10^{-5}, while the gap between asymptotic and simulated performance is 1.25 dB.

As presented in Fig. 8, different combiners with a slight impulsive noise are compared. For linear combiners SC, EGC and MRC, the threshold and numerical closed-form prediction are given and again closely match with the simulation results. We observe that the coded BEP of different combining methods agrees with the uncoded BEP obtained in the above section, where MRC still outperforms SC and EGC for slightly impulsive channels. Meanwhile, the non-linear detectors outperform the linear combiners. The performance of the optimal detector and our proposed detector are almost the same, which is 0.7 dB better than MRC and the Cauchy detector.

The performance of SC with exact and estimated α and γ is presented in Fig. 9. The curves named "sim. no est." and "sim. est." represent simulation results with known and estimated parameters, respectively. In our experiments, the average estimation errors of α are $8\%, 6\%$ and 4% at $N = 1000, 4000$ and 20000, respectively. The corresponding average estimation

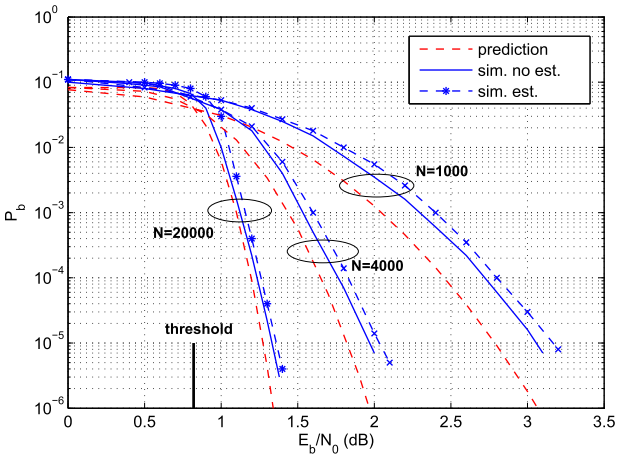

Fig. 9. Performance of irregular LDPC-coded SC with exact and estimated parameters on Rayleigh fading channels with SαS noise at $\alpha = 1.5$ and $L_r = 3$.

errors of γ are $16\%, 17\%$ and 18% at $E_b/N_0 = 0$ dB ($\gamma = 0.64$). As shown in Fig. 9, the difference between the performance with known parameters and the performance with estimated parameters is small, being less than 0.1 dB. It implies that the LDPC decoder is very robust against estimation errors.

We observe that the waterfall region prediction of LDPC codes becomes more accurate as N increases. The reasons are as follows: first, the P_{th} obtained from DE assume the LDPC code is cycle-free and the block length is infinite. However, the effect of cycles can not be avoid and it becomes more serious at short block length which degrades performance. The prediction of waterfall region is more accurate at long block length since the concentration theorem states that the average behavior of individual LDPC codes converges to the cycle-free case as the block length grows [39]. Second, the Gaussian approximation might be a source of inaccuracy since according to central limit theorem (CLT), the pdf of P^{α}_{obs} converges to Gaussian pdf only when N is large.

To numerically evaluate the accuracy of the Gaussian approximation, the Kullback-Leibler (KL) divergence is employed to calculate the difference between the two pdfs. KL divergence is defined as $D_{\text{KL}}(P||Q) = \sum_i P(i) \log \frac{P(i)}{Q(i)}$, where P is the true pdf and Q is an approximation of P. In our case, P is the binomial pdf $B(N, P^c_{b,\alpha})$ and Q is the normal distribution $\mathcal{N}(P^c_{b,\alpha}, P^c_{b,\alpha}(1 - P^c_{b,\alpha})/N)$. It is obvious that P and Q are determined by N and $P^c_{b,\alpha}$ which is related to α. In order to examine the influence of N and α on the accuracy of the approximation, we take Fig. 6 and Fig. 9 as examples. As shown in Fig. 6, the channel is extremely impulsive with $\alpha = 0.6$. $N = 1000, 4000, 20000$ and $P^c_{b,\alpha}$ can be calculated by (24). We note that this approximation generally improves as N increases and $P^c_{b,\alpha}$ is not near to 0 or 1 [43]. Hence, in order to investigate the validity of Gaussian approximation, for the worst case, we choose the smallest $P^c_{b,\alpha} = 0.0948$ which can be calculated from (24) at $E_b/N_0 = 16$ dB in Fig. 6. Hence the KL divergence between the pdf of P^{α}_{obs} and Gaussian distribution is obtained as $6.4\times10^{-4}, 1.6\times10^{-4}, 3.2\times10^{-5}$ for $N = 1000, 4000, 20000$, respectively. Similarly, as shown in Fig. 9, when the channel is moderate impulsive ($\alpha = 1.5$), the KL divergence at $E_b/N_0 = 3$ dB is obtained as $9.2 \times 10^{-4}, 2.3 \times 10^{-4}, 4.6 \times 10^{-5}$ for $N = 1000, 4000, 20000$, respectively. Hence, the Gaussian approximation is very accurate even for short length LDPC codes ($N = 1000$), since the KL divergence is very small. In addition, the value of α has little impact on the accuracy of approximation. The reason is the LDPC-coded performance is much better than uncoded performance for each α, which will result in a relatively large $P^c_{b,\alpha}$ at the range of E_b/N_0.

VI. Conclusion

In this paper, we investigate the uncoded and coded performance of linear diversity combining schemes on Rayleigh fading channels with independent SαS noise. The asymptotic performance of LDPC codes is derived using DE to verify the effectiveness of our analysis. In addition, a closed-form expression of the waterfall performance is given that reduces the gap between the asymptotic and simulated performance of LDPC codes. As discussed in the results section, MRC is not the best linear combiner, especially when the channel becomes more impulsive, and SC shows superior performance when the effect of impulses is very strong. An interesting result is when the channel is very impulsive, more branches have no benefit and can even degrade the performance with EGC and MRC. Meanwhile, non-linear detectors show a better performance than linear combiners with higher complexity and we proposed a reduced complexity detector by approximating the SαS pdf through a closed-form BCGM pdf which can achieve near optimal performance for all α.

VII. *Appendix A
The distribution of combined noise for EGC

The combined noise in (21) is expressed as

$$n_{\text{egc}} = \sum_{l=1}^{L_r} \tilde{n}_l \tag{55}$$

where $\tilde{n}_l = n_l e^{-j\phi_l}$ and n_l is an independently complex SαS random variables. Hence, according to (4), $\tilde{n}_l$ can be written as

$$\begin{aligned} \tilde{n}_l &= \sqrt{B_1} G_1 e^{-j\phi_l} + j\sqrt{B_2} G_2 e^{-j\phi_l} \\ &= \sqrt{B_1} G_1^{'} + j\sqrt{B_2} G_2^{'}, \end{aligned} \tag{56}$$

where $G_1^{'} = G_1 e^{-j\phi_l}$ and $G_2^{'} = G_2 e^{-j\phi_l}$. According to the isotropic property of Gaussian random variables, $G_1^{'}$ and $G_1^{'}$ are also Gaussian with the same mean and variance as G_1 and G_2. Hence $\tilde{n}_l$ also follows SαS distribution with the same α and γ as n_l.

Appendix B
The relationship of the dispersion between SC, MRC and EGC

First, we prove that $\gamma_{\text{mrc}} \leq \hat{\gamma}_{\text{egc}}$ for $0 < \alpha < 2$. According to the power mean inequality, for real numbers k_1, k_2 and

positive real numbers $a_1, a_2, \cdots, a_n$, $k_1 \leq k_2$ implies that

$$\left(\frac{\sum_{i=1}^{n} a_i^{k_1}}{n}\right)^{\frac{1}{k_1}} < \left(\frac{\sum_{i=1}^{n} a_i^{k_2}}{n}\right)^{\frac{1}{k_2}}. \tag{57}$$

Hence, in our case, we can obtain

$$\left(\sum_{l=1}^{L_r} a_l^{\alpha}\right)^{\frac{1}{\alpha}} \leq L_r^{\frac{1}{\alpha}-\frac{1}{2}} \left(\sum_{l=1}^{L_r} a_l^2\right)^{\frac{1}{2}}. \tag{58}$$

For MRC, by substituting (58) to (30), we can write

$$\gamma_{\text{mrc}} \leq \frac{L_r^{\frac{1}{\alpha}-\frac{1}{2}}}{\left(\sum_{l=1}^{L_r} a_l^2\right)^{\frac{1}{2}}}\gamma \leq \frac{L_r^{\frac{1}{\alpha}}}{\left(\sum_{l=1}^{L_r} a_l\right)}\gamma = \hat{\gamma}_{\text{egc}}. \tag{59}$$

For EGC, one obtains

$$\hat{\gamma}_{\text{egc}} = \frac{L_r^{1/\alpha}}{\sum_{l=1}^{L_r} a_l}\gamma \leq \frac{L_r^{1/\alpha}}{a_m}\gamma = L_r^{1/\alpha}\hat{\gamma}_{\text{sc}}. \tag{60}$$

When $0 < \alpha \leq 1$, it was proved that $\hat{\gamma}_{\text{sc}} \leq \gamma_{\text{mrc}}$ in [21]. Hence, the relationship of linear combiners is given as

$$\hat{\gamma}_{\text{sc}} \leq \gamma_{\text{mrc}} \leq \hat{\gamma}_{\text{egc}} \leq L_r^{1/\alpha}\hat{\gamma}_{\text{sc}}. \tag{61}$$

When $1 \leq \alpha < 2$, $\hat{\gamma}_{\text{sc}}$ is not always less than γ_{mrc}. With the help of (57), the relationship is derived as

$$\begin{aligned}\gamma_{\text{mrc}} &\geq \frac{\sum_{l=1}^{L_r} a_l}{\sum_{l=1}^{L_r} a_l^2} L_r^{\frac{1}{\alpha}-1}\gamma \\ &\geq \frac{\sum_{l=1}^{L_r} a_l}{\sum_{l=1}^{L_r} a_l a_m} L_r^{\frac{1}{\alpha}-1}\gamma \\ &= \frac{1}{a_m} L_r^{\frac{1}{\alpha}-1}\gamma = L_r^{\frac{1}{\alpha}-1}\hat{\gamma}_{\text{sc}}.\end{aligned} \tag{62}$$

Hence, the relationship of the dispersion for SC, MRC and EGC when $1 \leq \alpha < 2$ is

$$L_r^{\frac{1}{\alpha}-1}\hat{\gamma}_{\text{sc}} \leq \gamma_{\text{mrc}} \leq \hat{\gamma}_{\text{egc}} \leq L_r^{1/\alpha}\hat{\gamma}_{\text{sc}}. \tag{63}$$

REFERENCES

[1] D. Middleton, "Non-Gaussian noise models in signal processing for telecommunications: New methods an results for class A and class B noise models," *IEEE Trans. Inf. Theory*, vol. 45, no. 4, pp. 1129–1149, May 1999.

[2] K. Gulati, A. Chopra, R. W. Heath, Jr., B. L. Evans, K. R. Tinsley, and X. E. Lin, "MIMO receiver design in the presence of radio frequency interference," in *Proc. IEEE Global Commun. Conf. (GLOBECOM)*, Mar. 2008, pp. 1–5.

[3] H. El Ghannudi, L. Clavier, N. Azzaoui, F. Septier, and P. A. Rolland, "α-stable interference modeling and cauchy receiver for an IR-UWB Ad Hoc network," *IEEE Trans. Commun.*, vol. 58, no. 6, pp. 1748–1757, Jun. 2010.

[4] M. Nassar, K. Gulati, M. R. DeYoung, B. L. Evans, and K. R. Tinsley, "Mitigating near-field interference in laptop embedded wireless transceivers," *J. Signal Process. Syst.*, vol. 63, no. 1, pp. 1–12, 2011.

[5] M. Chitre, J. Potter, and O. S. Heng, "Underwater acoustic channel characterisation for medium-range shallow water communications," in *Proc. MTTS/IEEE TECHNO-OCEAN*, vol. 1. Nov. 2004, pp. 40–45.

[6] A. Nasri, R. Schober, and Y. Ma, "Unified asymptotic analysis of linearly modulated signals in fading, non-Gaussian noise, and interference," *IEEE Trans. Commun.*, vol. 56, no. 6, pp. 980–990, Jun. 2008.

[7] J. Ilow and D. Hatzinakos, "Analytic alpha-stable noise modeling in a Poisson field of interferers or scatterers," *IEEE Trans. Signal Process.*, vol. 46, no. 6, pp. 1601–1611, Jun. 1998.

[8] K. Gulati, B. L. Evans, J. G. Andrews, and K. R. Tinsley, "Statistics of Co-channel interference in a field of poisson and poisson-poisson clustered interferers," *IEEE Trans. Signal Process.*, vol. 58, no. 12, pp. 6207–6222, Dec. 2010.

[9] A. Chopra and B. L. Evans, "Joint statistics of radio frequency interference in multiantenna receivers," *IEEE Trans. Signal Process.*, vol. 60, no. 7, pp. 3588–3603, Oct. 2012.

[10] A. Chopra and B. L. Evans, "Outage probability for diversity combining in interference-limited channels," *IEEE Trans. Wireless Commun.*, vol. 12, no. 2, pp. 550–560, Feb. 2013.

[11] A. Rajan and C. Tepedelenlioğlu, "Diversity combining over Rayleigh fading channels with symmetric alpha-stable noise," *IEEE Trans. Wireless Commun.*, vol. 9, no. 9, pp. 2968–2976, Dec. 2010.

[12] M. A. Chitre, J. R. Potter, and S. H. Ong, "Optimal and near-optimal signal detection in snapping shrimp dominated ambient noise," *IEEE J. Ocean. Eng.*, vol. 31, no. 2, pp. 497–503, Apr. 2006.

[13] S. Niranjayan and N. C. Beaulieu, "A myriad filter detector for UWB multiuser communication," in *Proc. IEEE Int. Conf. Commun. (ICC)*, Mar. 2008, pp. 3918–3922.

[14] A. Mahmood, M. Chitre, and M. A. Armand, "PSK communication with passband additive symmetric α-stable noise," *IEEE Trans. Commun.*, vol. 60, no. 10, pp. 2990–3000, Oct. 2012.

[15] G. A. Tsihrintzis and C. L. Nikias, "Performance of optimum and suboptimum receivers in the presence of impulsive noise modeled as an alpha-stable process," *IEEE Trans. Commun.*, vol. 43, no. 2, pp. 904–914, Feb. 1995.

[16] D. H. Johnson, "Optimal linear detectors for additive noise channels," *IEEE Trans. Signal Process.*, vol. 44, no. 12, pp. 3079–3084, Dec. 1996.

[17] A. Mahmood, M. Chitre, and M. A. Armand, "On single-carrier communication in additive white symmetric alpha-stable noise," *IEEE Trans. Commun.*, vol. 62, no. 10, pp. 3584–3599, Oct. 2014.

[18] A. Mahmood, M. Chitre, and M. A. Armand, "Detecting ofdm signals in alpha-stable noise," *IEEE Trans. Commun.*, vol. 62, no. 10, pp. 3571–3583, Oct. 2014.

[19] F. Yang and X. Zhang, "BER and SER analyses for M-ary modulation schemes under symmetric alpha-stable noise," in *Proc. IEEE Global Commun. Conf. (GLOBECOM)*, Dec. 2014, pp. 3983–3988.

[20] S. Niranjayan and N. C. Beaulieu, "The BER optimal linear rake receiver for signal detection in symmetric alpha-stable noise," *IEEE Trans. Commun.*, vol. 57, no. 12, pp. 3585–3588, Dec. 2009.

[21] S. Niranjayan and N. C. Beaulieu, "BER optimal linear combiner for signal detection in symmetric alpha-stable noise: Small values of alpha," *IEEE Trans. Wireless Commun.*, vol. 9, no. 3, pp. 886–890, Mar. 2010.

[22] S. Gounai and T. Ohtsuki, "Performance analysis of LDPC code with spatial diversity," in *Proc. IEEE Veh. Technol. Conf.*, Sep. 2006, pp. 1–5.

[23] B. S. Tan, K. H. Li, and K. C. Teh, "Performance analysis of LDPC codes with maximum-ratio combining cascaded with selection combining over Nakagami-m fading," *IEEE Trans. Wireless Commun.*, vol. 10, no. 6, pp. 1886–1894, Jun. 2011.

[24] C. Di, D. Proietti, I. E. Telatar, T. J. Richardson, and R. L. Urbanke, "Finite-length analysis of low-density parity-check codes on the binary erasure channel," *IEEE Trans. Inf. Theory*, vol. 48, no. 6, pp. 1570–1579, Jun. 2002.

[25] A. Amraoui, A. Montanari, T. Richardson, and R. Urbanke, "Finite-length scaling for iteratively decoded LDPC ensembles," *IEEE Trans. Inf. Theory*, vol. 55, no. 2, pp. 473–498, Feb. 2009.

[26] R. Yazdani and M. Ardakani, "An efficient analysis of finite-length LDPC codes," in *Proc. IEEE Int. Conf. Commun. (ICC)*, Oct. 2007, pp. 677–682.

[27] M. Noor-A-Rahim, K. D. Nguyen, and G. Lechner, "Finite length analysis of LDPC codes," in *Proc. IEEE Wireless Commun. Netw. Conf. (WCNC)*, Apr. 2014, pp. 206–211.

[28] X. Li, J. Sun, L. Jin, and M. Liu, "Bi-parameter CGM model for approximation of a-stable PDF," *Electron. Lett.*, vol. 44, no. 18, pp. 1096–1097, 2008.

[29] M. Shao and C. L. Nikias, "Signal processing with fractional lower order moments: Stable processes and their applications," *Proc. IEEE*, vol. 81, no. 7, pp. 986–1010, Jul. 1993.

[30] G. Samoradnitsky and M. S. Taqqu, *Stable Non-Gaussian Random Processes: Stochastic Models with Infinite Variance*. London, U.K.: Chapman & Hall, 1994.

[31] J. H. McCulloch, "Simple consistent estimators of stable distribution parameters," *Commun. Statist.-Simul. Comput.*, vol. 15, no. 4, pp. 1109–1136, 1986.
[32] G. A. Tsihrintzis and C. L. Nikias, "Fast estimation of the parameters of alpha-stable impulsive interference," *IEEE Trans. Signal Process.*, vol. 44, no. 6, pp. 1492–1503, Jun. 1996.
[33] E. E. Kuruoglu, "Density parameter estimation of skewed α-stable distributions," *IEEE Trans. Signal Process.*, vol. 49, no. 10, pp. 2192–2201, Mar. 2001.
[34] J. G. Gonzalez, J. L. Paredes, and G. R. Arce, "Zero-order statistics: A mathematical framework for the processing and characterization of very impulsive signals," *IEEE Trans. Signal Process.*, vol. 54, no. 10, pp. 3839–3851, Oct. 2006.
[35] J. P. Nolan, "Numerical calculation of stable densities and distribution functions," *Commun. Statist. Stochastic Models*, vol. 13, no. 4, pp. 759–774, 1997.
[36] M. Schwartz, W. R. Bennett, and S. Stein, *Communication Systems and Techniques*. Hoboken, NJ, USA: Wiley, 1995.
[37] J. Hu and N. C. Beaulieu, "Accurate simple closed-form approximations to Rayleigh sum distributions and densities," *IEEE Commun. Lett.*, vol. 9, no. 2, pp. 109–111, Feb. 2005.
[38] H. B. Mâad, A. Goupil, L. Clavier, and G. Gelle, "Asymptotic performance of LDPC codes in impulsive non-Gaussian channel," in *Proc. IEEE 11th Int. Workshop Signal Process. Adv. Wireless Commun. (SPAWC)*, Jun. 2010, pp. 1–5.
[39] T. J. Richardson and R. L. Urbanke, "The capacity of low-density parity-check codes under message-passing decoding," *IEEE Trans. Inf. Theory*, vol. 47, no. 2, pp. 599–618, Feb. 2001.
[40] S.-Y. Chung, T. J. Richardson, and R. L. Urbanke, "Analysis of sum-product decoding of low-density parity-check codes using a Gaussian approximation," *IEEE Trans. Inf. Theory*, vol. 47, no. 2, pp. 657–670, Feb. 2001.
[41] S. ten Brink, G. Kramer, and A. Ashikhmin, "Design of low-density parity-check codes for modulation and detection," *IEEE Trans. Commun.*, vol. 52, no. 4, pp. 670–678, Apr. 2004.
[42] X.-Y. Hu, E. Eleftheriou, and D. M. Arnold, "Regular and irregular progressive edge-growth tanner graphs," *IEEE Trans. Inf. Theory*, vol. 51, no. 1, pp. 386–398, Jan. 2005.
[43] G. E. Box *et al.*, *Statistics for Experimenters: An Introduction to Design, Data Analysis, and Model Building*. New York, NY, Wiley: 1978.

Zhen Mei received the B.Eng. degree in electronics and information engineering from Central China Normal University, China, in 2012, and the M.Sc. degree in communications and signal processing from Newcastle University, U.K., in 2013, where he is currently pursuing the Ph.D. degree with the School of Electrical and Electronic Engineering. His research interests include channel coding, wireless communications, and impulsive noise.

Martin Johnston received the B.Sc. degree (Hons.) in physics with electronics from Birmingham University, U.K., in 1999, the M.Sc. degree in electronic engineering from Staffordshire University, U.K., in 2001, and the Ph.D. degree from Newcastle University, U.K., in 2006. From 2006 to 2014, he was a Research Associate with the School of Electrical and Electronic Engineering, Newcastle University, where he is currently a Lecturer. His research interests include the design of advanced error-correcting schemes and low-complexity decoding algorithms, physical layer network coding, and physical layer security.

Stéphane Le Goff received the B.Sc., M.Sc., and Ph.D. degrees in electrical engineering from the Université de Bretagne Occidentale (University of Western Brittany), Brest, France, in 1990, 1991, and 1995, respectively. From 1995 to 1998, he was an Adjunct Lecturer with the Institut Supérieur d'Electronique de Bretagne, a French college of electronic engineering. From 1999 to 2003, He was an Assistant Professor with the Etisalat College of Engineering, UAE. In 2003, he joined the Department of Physics and Electronics, University of Waikato, Hamilton, New Zealand, as a Senior Lecturer in Electronics. He also held visiting positions at Eastern Mediterranean University, Cyprus, from 1998 to 1999 and Sultan Qaboos University, Oman, in 2004. Since 2005, he has been a Lecturer with the School of Electrical, and Electronic Engineering, Newcastle University, U.K. His research interests include information theory, channel coding, and wireless communication systems.

Li Chen (S'07–M'08–SM'14) received the B.Sc. degree in applied physics from Jinan University, China, in 2003, and the M.Sc. degree in communications and signal processing and the Ph.D. degree in communications engineering from Newcastle University, U.K., in 2004 and 2008, respectively. From 2007 to 2010, he was a Research Associate with Newcastle University. In 2010, he was a Lecturer with the School of Information Science and Technology, Sun Yat-sen University, China, where he became an Associate Professor in 2011. Since 2016, he has been a Professor with the School of Electronics and Information Engineering, Sun Yat-sen University. From 2011 to 2012, he was an occasional Visiting Scholar with the Institute of Network Coding, The Chinese University of Hong Kong. In 2015, he was a Visitor at the Institute of Communication Engineering, Ulm University, Germany. From 2015 to 2016, he was a Visiting Associate Professor with the Department of Electrical Engineering, University of Notre Dame, USA. His primary research interests include information theory, channel coding, and data communications. He was a recipient of the British Overseas Research Scholarship and the Chinese Information Theory Young Researcher in 2014. He has been a Principle Investigator for three National Natural Science Foundation of China projects and a Co-Investigator of a National Basic Research Program (973 program) Project.